Dokuz Eylül Üniversitesi-Mühendislik Fakültesi
Fen ve Mühendislik Dergisi
Cilt 20, Sayı 59 , Mayıs, 2018

Dokuz Eylul University-Faculty of Engineering
Journal of Science and Engineering
Volume 20, Issue 59, May, 2018

DOI: 10.21205/deufmd. 2018205946

Critical Buckling Load Analysis of Layered Functionally Graded Shell Structures

Savas EVRAN[*1]

[1]Canakkale Onsekiz Mart University, Vocational School of Canakkale Technical Sciences, Department of Machine and Metal Technologies, 17020, Canakkale
http://orcid.org/0000-0002-7512-5997)

(Alınış / Received: 31.10.2017, Kabul / Accepted: 19.01.2018,
Online Yayınlanma / Published Online: 15.05.2018)

Keywords
Shell Structures, Functionally Graded Materials, Buckling, Finite Element Method

Abstract: In this study, critical buckling load analysis for first mode of layered functionally graded shell structures made of silicon nitride (Si_3N_4)/stainless steel (SUS304) systems is studied. The shell structures are considered as three layers and the layer positions are carried out according to L9 (3^3) orthogonal array. The mechanical properties of the layers are calculated according to a simple rule of mixture of composite materials. The mechanical properties of the layers is assumed to be control factors. Optimum layer levels are obtained using signal to noise (S/N) analysis. Significant layers and their percent contributions on the results are detected using analysis of variance (ANOVA). Maximum buckling load value is carried out based on different arrangements of optimum layer levels.

Tabakalı Fonksiyonel Derecelendirilmiş Kabuk Yapıların Kritik Burkulma Yükü Analizi

Anahtar Kelimeler
Kabuk Yapılar, Fonksiyonel Derecelendirilmiş Malzemeler, Burkulma, Sonlu Elemanlar Yöntemi

Öz: Bu çalışmada, silisyum nitrür (Si_3N_4)/paslanmaz çelik (SUS304) sistemlerinden yapılmış tabakalı fonksiyonel derecelendirilmiş kabuk yapıların birinci mod için kritik burkulma yük analizi çalışılmıştır. Kabuk yapılar üç tabakalı olarak düşünülmüş ve tabaka pozisyonları L9 (3^3) ortogonal diziye göre gerçekleştirilmiştir. Tabakaların mekanik özellikleri, kompozit malzeme karışımının basit kuralına bağlı olarak hesaplanmıştır. Tabakaların mekanik özellikleri kontrol faktörleri olarak kabul edilmiştir. Optimum tabaka seviyeleri sinyal gürültü (S/N) analizi kullanılarak elde edilmiştir. Sonuçlar üzerinde önemli tabakalar ve onların yüzde katkıları varyans analizi (ANOVA) kullanılarak tespit edilmiştir. Maksimum burkulma yük değeri optimum tabakaların farklı sıralamasına bağlı gerçekleştirilmiştir.

*Sorumlu yazar: sevran@comu.edu.tr

1. Introduction

In the mechanical engineering fields, structures made of various type materials such as metal, ceramic, plastic, composite etc. are used in different application areas. Especially, composite materials has a wide range of uses. It is possible to see Functionally Graded Materials (FGMs) in many various application fields of mechanical engineering as a new kind of composite materials. These materials can be generally made using superior features of different materials and so the new structures with superior features can be designed to adapt to different environmental conditions. In recent years, many researches have been made using the new type of composite called FGMs. This materials are submitted by a few scientists interested material science in Sendai region of Japan, 1984 [1]. FGMs generally consist of a mixture obtained using metal and ceramic materials and are composite materials with heterogeneous structure [2]. In literature, many studies consisting of the buckling analysis of structures made of FGMs have been published. Shariat and Eslami [3] performed the buckling behavior of plates consisting of functionally graded materials according to thermal and mechanical loads and the mechanical properties of these plates were changed in the thickness direction linearly. In addition, they selected the rectangular thick plates in the analyses. Li and Batra [4] evaluated the buckling behavior of circular cylindrical shell consisting of three layers under simply supported boundary condition based on axial compressive load and the circular cylindrical shell is considered as functionally graded middle layer. Zhao et al. [5] observed the buckling behavior of plates with functionally graded materials obtained using ceramic and metal materials towards thickness direction under mechanical and thermal loads. Feldman and Aboudi [6] examined the buckling behavior of plates designed using functionally graded materials according to uniaxial loading. Huang and Han [7] reported a study consisting of the buckling analysis of imperfect cylindrical shell prepared using functionally graded materials based on axial compression loading. Ramu and Mohanty [8] carried out the buckling behavior of plates designed using functionally graded materials according to uniaxial and biaxial compressions and the plates were considered as rectangular. Silicon nitride and stainless steel materials were used in analyses. Mohammadi et al. [9] reported an analytical approach named Levy for buckling behavior of plates made using FGM and the mechanical properties of the plates were considered to be varied continuously towards thickness direction. The shapes of the plates assumed as thin and rectangular. Javaheri and Eslami [10] observed the buckling behavior of plates prepared using FGM according to in-plane compressive loading. Reddy et al. [11] carried out the buckling response of plates consisting of functionally graded materials using metal and ceramic in thickness direction under simply supported boundary condition according to higher order shear deformation theory. Mahdavian [12] evaluated the buckling response of the plates prepared using functionally graded materials under simply supported boundary condition according to uniform in-plane compression and the plates were considered as rectangular shape. Sepiani et al. [13] examined the free vibration and buckling behaviors of cylindrical shell consisting of two layers under combined static and periodic axial loading and the shell layers assumed to be inner layer and out layer consisting of functionally graded materials and isotropic elastic

respectively. Saha and Maiti [14] observed the buckling responses of plates formed using functionally graded materials obtained using metal and ceramic mixture subjected to uniaxial loading based on simply supported boundary condition and alumina and aluminium were used metal and ceramic respectively. Bodaghi and Saidi [15] submitted an analytical solution called Levy-type for buckling behavior of plates formed using FGM based on the higher-order shear deformation plate theory and the plates were considered as thick and rectangular shapes. Bagherizadeh et al. [16] examined the buckling response of cylindrical shells designed using FGM for mechanical loading and the shells were surrounded based on pasternak elastic foundation. Mozafari and Ayob [17] studied the influence of thickness variation for critical buckling loads of plates consisting of functionally graded materials using ceramic and metal materials. The buckling analyses were performed according to in-plane compression. Oyekoya et al. [18] evaluated the buckling and vibration behaviors of composite structures prepared from functionally graded materials according to the finite element theory. In the presented work, critical buckling load of layered functionally graded shell structures was analyzed based on the finite element software ANSYS V13 and L9 orthogonal array with nine runs and three control factors.

2. Material and Method

2.1. Materials

Numerical analyses of the layered functionally graded shell structures in z axis direction, made of three layers, are carried out based on systems consisting of ceramic and metal materials. Silicon nitride (Si_3N_4) and stainless steel (SUS304) are determined as ceramic and metal materials respectively. These materials were used in another study [8] to prepare the rectangular plate. Mechanical properties of the materials are illustrated in Figure 1.

Table 1. Mechanical properties [19]

Properties	Unit	Materials	
		Si_3N_4	SUS304
Young's Modulus (E)	GPa	322.27	207.78
Poisson's ratio (ν)	-	0.24	0.3177

2.2. Methods

Layer arrangements of the layered functionally graded shell structures are performed using L9 orthogonal array with three control factors and three levels according to Taguchi Method. Layers are made of different volume fractions of the materials, based on the increments of 9% Si_3N_4 ceramic material. Layers are considered as control factor. The control factors and their levels are given in Table 2.

Table 2. Control factors and levels

Levels	Control Factors		
	Layer1	Layer2	Layer3
Level 1	9%Si_3N_4-91%SUS304	36%Si_3N_4-64%SUS304	63%Si_3N_4-37%SUS304
Level 2	18%Si_3N_4-82%SUS304	45%Si_3N_4-55%SUS304	72%Si_3N_4-28%SUS304
Level 3	27%Si_3N_4-73%SUS304	54%Si_3N_4-46%SUS304	81%Si_3N_4-19%SUS304

Each control factor is assumed to be layer consisting of different volume fractions of Si_3N_4 and SUS304 materials and so each layer has various mechanical properties. The material properties of layers are achieved using a simple rule of mixture of composite materials. The Layers' effective

mechanical properties (P_{ef}) such as Young's Modulus (E_f), and poisson's ratio (ν_f) can be calculated using Equation [20].

$$P_{ef} = \sum_{i=1} P_i V_{f_i} \quad (1)$$

where, P_i and V_{fi} are used as the mechanical properties and volume fraction of the constituent material i respectively. The sum of the volume fractions of all the constituent materials becomes one as given in Equation 2 [20].

$$\sum_{i=1} V_{f_i} = 1 \quad (2)$$

Mechanical properties calculated using Equation 1 and 2 are taken as control factors and the layered functionally graded shell structures are modelled based on L9 orthogonal array. The numeric results are analyzed in Minitab R15 software according to "Higher is better" type quality characteristic as shown in Equation 3 [22].

$$(S/N)_{HB} = -10.log\left(n^{-1}\sum_{i=1}^{n}(y_i^2)^{-1}\right) \quad (3)$$

where, n presents number of test in a trial and y_i illustrates the investigated ith data.

3. Finite Element Analysis

Numerical analyses are performed using finite element software ANSYS V13 Mechanical APDL. SHELL281 with eight-node is used in analysis and the element is convenient using analyzing thin to moderately-thick shell structures. Mesh operations are performed using 100x100 elements under mapped mesh. Shell structures have three layers and each layer is assumed to be square shape as 200x200 mm^2 and 3 mm thickness. Layer arrangements are performed in the z axis direction. In the analyses, degrees of freedom is determined as UX, UY, UZ, ROTX, ROTY and ROTZ. Block Lanczos is selected for extraction method. Analyses are performed under clamped-free-free-free (CFFF) boundary conditions. Pressure is applied on the top side using 1 value and results obtained are multiplied by 200 value, known as side length layered functionally graded shell structures. Clamped end is selected to be bottom side as shown in Figure 1.

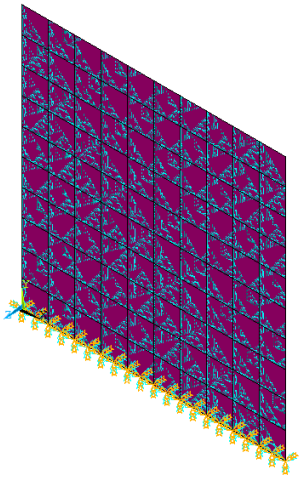

Figure 1. Layered functionally graded shell structure with clamped-free-free-free (CFFF)

4. Numerical Results and Discussion

Critical buckling analysis of layered shell structures consisting of functionally graded materials are observed to determine optimum layer levels, layer effects and maximum critical load values on the layered functionally graded shell structures made of metal and ceramic. The numerical results are investigated for first mode of the shell structures. S/N ratio values for results are calculated using Minitab R15 software according to Equation 3. The results and their S/N ratio values are tabled in Table 3.

Table 3. Critical buckling loads and S/N ratio results

Runs	Control Factors			Results	
	Layer1	Layer2	Layer3	P (N)	η (dB)
1	9%Si_3N_4-91%SUS304	36%Si_3N_4-64%SUS304	63%Si_3N_4-37%SUS304	194236	105.767
2	9%Si_3N_4-91%SUS304	45%Si_3N_4-55%SUS304	72%Si_3N_4-28%SUS304	197650	105.918
3	9%Si_3N_4-91%SUS304	54%Si_3N_4-46%SUS304	81%Si_3N_4-19%SUS304	200998	106.064
4	18%Si_3N_4-82%SUS304	36%Si_3N_4-64%SUS304	72%Si_3N_4-28%SUS304	201610	106.090
5	18%Si_3N_4-82%SUS304	45%Si_3N_4-55%SUS304	81%Si_3N_4-19%SUS304	205028	106.236
6	18%Si_3N_4-82%SUS304	54%Si_3N_4-46%SUS304	63%Si_3N_4-37%SUS304	199053	105.979
7	27%Si_3N_4-73%SUS304	36%Si_3N_4-64%SUS304	81%Si_3N_4-19%SUS304	208958	106.401
8	27%Si_3N_4-73%SUS304	45%Si_3N_4-55%SUS304	63%Si_3N_4-37%SUS304	202824	106.142
9	27%Si_3N_4-73%SUS304	54%Si_3N_4-46%SUS304	72%Si_3N_4-28%SUS304	206396	106.294
Overall Mean				201861	

4.1. Optimum Layer Levels and Their Effects

Numerical critical buckling load results are performed using finite element software ANSYS. Nine shell structures are modelled based on Taguchi L9 orthogonal array. Average numerical load and their S/N ratio values for each level of the each layer based on raw data are given in Table 4.

Table 4. Response table of S/N ratios and means

Level	S/N Ratios (dB)			Means (N)		
	Layer1	Layer2	Layer3	Layer1	Layer2	Layer3
1	105.9	106.1	106.0	197628	201601	198704
2	106.1	106.1	106.1	201897	201834	201885
3	106.3	106.1	106.2	206059	202149	204995
Delta	0.4	0	0.3	8431	548	6290
Rank	1	3	2	1	3	2

It is seen from Table 4 that optimum layers are determined for third level of the all layers according to "higher is better" type quality characteristic. In order word, the maximum critical buckling load are calculated using third levels of the layers. In addition, the delta and rank values presents that Layer1, Layer3 and Layer2 have the greatest effects on the critical buckling load analysis, respectively. The average S/N values of critical buckling loads for each layer at levels 1, 2 and 3 are illustrated in Figure 2. According to Figure 2, the increasing of percent volume fractions of SUS304 materials in Layer1, Layer2 and Layer3 decreases the critical buckling loads. This situation can be explained by the Young's modulus of materials. The increasing of the ceramic materials in layers causes the increasing the critical buckling load results.

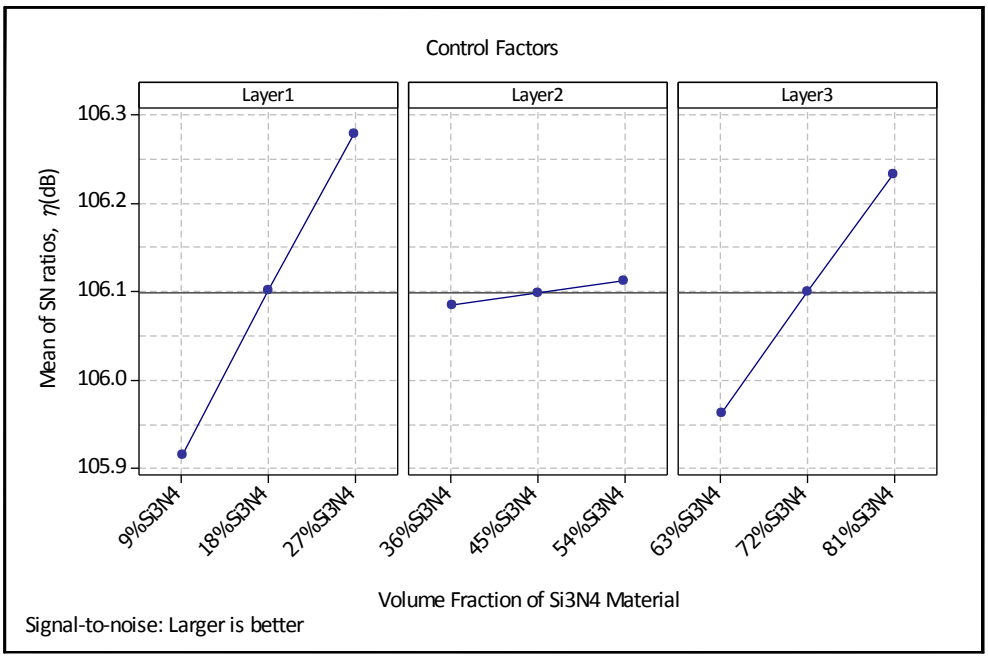

Figure 2. Main Influences Plot of S/N Ratios

4.2. Analysis of Variance

In order to carry out significant control factors and their percent effects on the critical buckling load results, Analysis of Variance (ANOVA) is performed for R-Sq = 99.99% and R-Sq(adj) = 99.97%. Each control factor has two DF (degrees of freedom) and error variance is obtained as 5812 value. The ANOVA results obtained for raw data using Minitab R15 software are illustrated in Table 5.

Table 5. ANOVA results for critical buckling loads

Source	DF	Seq SS	Adj MS	F	P	% Effects
Layer1	2	106633375	53316687	9174.260	0.000	64.06
Layer2	2	453090	226545	38.980	0.025	0.27
Layer3	2	59352483	29676241	5106.420	0.000	35.66
Error	2	11623	5812			0.01
Total	8	166450570				100

According to ANOVA results obtained for 95% confidence level, all layers are determined as significant control factors on the response because p values are smaller than 0.05 value. In addition Layer1 and Layer3 have more importance than Layer2 because p value of Layer2 is higher than Layer1 and Layer3. The percent contributions of layers on the critical buckling loads are obtained as Layer1 with 64.06 %, Layer3 with 35.66% and Layer2 with 0.27% respectively.

4.3. Estimation of Optimum Quality Characteristic

The optimal result of the first mode critical buckling load is predicted using the optimal levels of the important control parameters such as Layer1, Layer2 and Layer3 only. In order word, the optimum result of critical buckling

load is predicted according to the optimum levels of significant layers. The estimated mean of the first mode critical buckling load can be calculated using Equation 4 [21].

$$\widehat{\mu_{\mathrm{Pcr}}} = \bar{T}_{\mathrm{Pcr}} + (\overline{Layer1}_3 - \bar{T}_{\mathrm{Pcr}}) + (\overline{Layer2}_3 - \bar{T}_{\mathrm{Pcr}}) + (\overline{Layer3}_3 - \bar{T}_{\mathrm{Pcr}}) \quad (4)$$

where, $\bar{T}_{\mathrm{Pcr}}$=201861 represent the average mean of the first mode critical buckling load according to L9 orthogonal array and is obtained from Table 3. $\overline{Layer1}_3$=206059, $\overline{Layer2}_3$=202149 and $\overline{Layer1}_3$=204995 are determined as the average value of the first mode critical buckling load at level 3 and these values are obtained from Table 4. According to Equation 4, $\widehat{\mu_{\mathrm{Pcr}}}$ is computed as 209481 N. The 95% confidence intervals (CI) of confirmation buckling analysis (CI_{CBA}) is detected using Equation 5 [22].

$$CI_{\mathrm{CBA}} = \left(F_{\alpha;1;n_2} V_{error} \left[\frac{1}{n_{eff}} + \frac{1}{R} \right] \right)^{1/2} \quad (5)$$

in which, $F_{\alpha;1;n_2}$ represent the F value and n_2 is error data of (degree of freedom) and so $F_{0.05;1;2}$=18.513 is found from F data [21]. V_{error} =5812 is error value of variance is obtained from Table 5. R is considered as number of replications for confirmation buckling analysis and is taken as 1. n_{eff} means the effective number of replications and is detected using Equation 6 [22].

$$n_{eff}=N/(1+T_{DOF}) \quad (6)$$

in which, T_{DOF} is the total DF for significant control parameters is calculated as 6. This value are obtained from Table 5 including ANOVA results. N value represents the total number of the buckling analysis in Table 3 and N is used as 9. Thus the CI_{CBA} result obtained using Equation 4 and 5 is calculated as 437.36. The predicted 95% confidence interval for first mode critical buckling load is determined using Equation 7 [22].

$$\widehat{\mu_{\mathrm{Pcr}}} - CI_{CBA} < \mu_{Pcr} < \widehat{\mu_{\mathrm{Pcr}}} + CI_{CBA} \quad (7)$$

ANSYS and predicted results of optimum critical buckling load for first mode are demonstrated in Table 6.

Table 6. Numerical and predicted results of critical buckling load

Shell Structure with Optimum Levels	ANSYS Result	Predicted Result	Predicted CI for 95% Confidence Level
$(Layer1)_3$-$(Layer2)_3$-$(Layer3)_3$	209588 N	209481 N	209044< $\mu_{(Pcr\ for\ N)}$ < 209918
	106.427 dB	106.423 dB	106.405< $\mu_{(Pcr\ for\ dB)}$ <106.441

4.4. Effects of Mesh Elements

Influences of mesh elements are investigated using layered functionally graded shell structure with optimum layers. Six different mesh types are selected. The results obtained are given in Table 7.

Table 7. Mesh element effects on critical buckling loads

Critical Buckling Load	Type of Mesh Element					
	100x100	50x50	40x40	25x25	20x20	10x10
P_{cr} (N)	209588	209588	209588	209592	209592	209608

It is seen from Table 7 that the increasing of mesh elements decreases the first mode critical buckling load values from a mesh of 10x10 elements to a mesh of 40x40 elements.

4.5. Determine of Optimum Layer Positions

In order to determine the optimum layer positions on the layered functionally graded shell structures, shell structures configurations with optimum layers are analyzed using finite element software ANSYS. Six shell structure configurations are used and each configuration has same mechanical properties as the other configurations. The shell structure configurations and their critical buckling load results are tabulated in Table 8.

Table 8. Shell structure configurations with optimum layers

Analyses	Configurations			P_{cr} (N)
1	$Layer1_3$	$Layer2_3$	$Layer3_3$	209588
2	$Layer1_3$	$Layer3_3$	$Layer2_3$	200622
3	$Layer2_3$	$Layer1_3$	$Layer3_3$	220768
4	$Layer2_3$	$Layer3_3$	$Layer1_3$	200662
5	$Layer3_3$	$Layer1_3$	$Layer2_3$	220768
6	$Layer3_3$	$Layer2_3$	$Layer1_3$	209588

It is seen from Table 8 that maximum critical buckling load values are obtained using configurations with $Layer2_3$-$Layer1_3$- $Layer3_3$ and $Layer3_3$-$Layer1_3$-$Layer2_3$ and is followed by configurations with $Layer1_3$-$Layer2_3$-$Layer3_3$ and $Layer3_3$-$Layer2_3$- $Layer1_3$ and configurations with $Layer1_3$-$Layer3_3$- $Layer2_3$ and $Layer2_3$-$Layer3_3$-$Layer1_3$ in order that. Although these configurations have same mechanical properties, various layer positions give different results. This situation shows that the layer positions on the layered functionally graded shell structures play important role. In addition, it can said that top and bottom layers with high Young's Modulus increase the first mode critical buckling loads whereas middle layers with low Young's Modulus decrease. In order word, top and bottom layers with ceramic-rich increase the critical buckling load whereas middle layers with metal-rich decrease. First six mode shapes for critical buckling load of configurations with $Layer2_3$-$Layer1_3$-$Layer3_3$ are demonstrated in Figure 3.

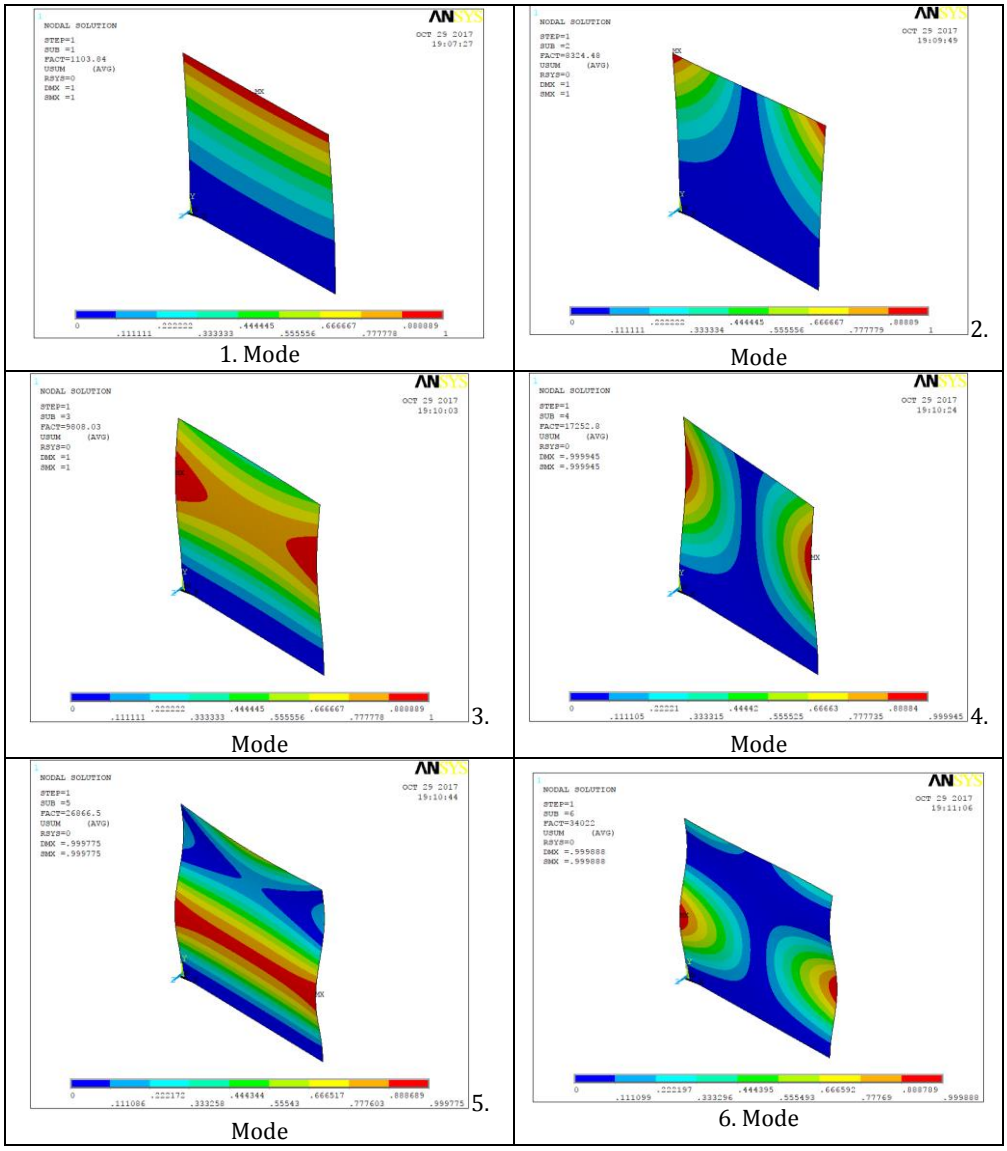

Figure 3. Different mode shapes of configurations with Layer2$_3$-Layer1$_3$- Layer3$_3$

5. Conclusion

In this study, critical buckling load analysis of functionally graded metal-ceramic shell structures consisting of three layers are investigated under mechanical loading using finite element software ANSYS V13 Mechanical APDL numerically. Layer arrangements of the shell structures in z axis direction are modelled based on L9 orthogonal array. In order to detect the maximum critical buckling load, various configurations with optimum layers are analyzed. According to this study:

- Maximum first mode critical buckling load is performed using third level of the layers under clamped-free-free-free boundary condition.
- The increasing of the volume fraction of ceramic materials causes the increasing the critical buckling loads.

- The most effective control parameters on the critical buckling loads for first mode are determined as Layer1 with 64.06%, Layer3 with 35.66% and Layer2 with 0.27 % effects, respectively.
- All layers have significant effects on the critical buckling loads for first mode since p values of the layers is smaller than 0.05 value at 95% confidence level according to ANOVA results.
- Top and bottom layers with ceramic-rich increase firs mode critical buckling loads whereas middle layers with metal-rich decrease.
- The 95% confidence interval of the predicted first mode critical buckling load is found to be $209044 < \mu_{(Pcr\ for\ N)} < 209918$.
- Mesh element numbers from 40x40 to 100x100 mesh elements have not significant influences on the critical buckling loads.
- The maximum critical buckling load for L9 orthogonal array is detected for configurations with $Layer1_3$-$Layer2_3$- $Layer3_3$ whereas is carried out using the configurations with $Layer2_3$-$Layer1_3$- $Layer3_3$ and $Layer3_3$- $Layer1_3$-$Layer2_3$ according to optimum layer positions

References

[1] Koizumi M. 1997. FGM activities in Japan, Composites Part B: Engineering, 28, 1997, p. 1-4.

[2] Singh JMS, Thangaratnam RK. 2010. Buckling and vibration analysis of FGM plates and shells. Frontiers in Automobile and Mechanical Engineering (FAME), 2010: IEEE; 2010. p. 280-285.

[3] Shariat BAS, Eslami MR. 2007. Buckling of thick functionally graded plates under mechanical and thermal loads, Composite Structures, 78, 2007, p. 433-439.

[4] Li S-R, Batra RC. 2006. Buckling of axially compressed thin cylindrical shells with functionally graded middle layer, Thin-Walled Structures, 44, 2006, p. 1039-1047.

[5] Zhao X, Lee YY, Liew KM. 2009. Mechanical and thermal buckling analysis of functionally graded plates, Composite Structures, 90, 2009, p. 161-171.

[6] Feldman E, Aboudi J. 1997. Buckling analysis of functionally graded plates subjected to uniaxial loading, Composite Structures, 38, 1997, p. 29-36.

[7] Huang H, Han Q. 2008. Buckling of imperfect functionally graded cylindrical shells under axial compression, European Journal of Mechanics - A/Solids, 27, 2008, p. 1026-1036.

[8] Ramu I, Mohanty SC. 2014. Buckling Analysis of Rectangular Functionally Graded Material Plates under Uniaxial and Biaxial Compression Load, Procedia Engineering, 86, 2014, p. 748-757.

[9] Mohammadi M, Saidi AR, Jomehzadeh E. 2010. Levy Solution for Buckling Analysis of Functionally Graded Rectangular Plates, Applied Composite Materials, 17, 2010, p. 81-93.

[10] Javaheri R, Eslami M. 2002. Buckling of Functionally Graded Plates under In-plane Compressive Loading, ZAMM-Journal of Applied Mathematics and Mechanics/Zeitschrift für Angewandte Mathematik und Mechanik, 82, 2002, p. 277-283.

[11] Reddy BS, Kumar JS, Reddy CE, Reddy KVK. 2013. Buckling Analysis of Functionally Graded Material Plates Using Higher Order Shear Deformation Theory, Journal of Composites, 2013, 2013, p. 1-12.

[12] Mahdavian M. 2009. Buckling analysis of simply-supported functionally graded rectangular

plates under non-uniform in-plane compressive loading, Journal of Solid Mechanics, 1, 2009, p. 213-225.

[13] Sepiani HA, Rastgoo A, Ebrahimi F, Ghorbanpour Arani A. 2010. Vibration and buckling analysis of two-layered functionally graded cylindrical shell, considering the effects of transverse shear and rotary inertia, Materials & Design, 31, 2010, p. 1063-1069.

[14] Saha R, Maiti P. 2012. Buckling of simply supported FGM plates under uniaxial load, International Journal of Civil and Structural Engineering, 2, 2012, p. 1035-1050.

[15] Bodaghi M, Saidi AR. 2010. Levy-type solution for buckling analysis of thick functionally graded rectangular plates based on the higher-order shear deformation plate theory, Applied Mathematical Modelling, 34, 2010, p. 3659-3673.

[16] Bagherizadeh E, Kiani Y, Eslami MR. 2011. Mechanical buckling of functionally graded material cylindrical shells surrounded by Pasternak elastic foundation, Composite Structures, 93, 2011, p. 3063-3071.

[17] Mozafari H, Ayob A. 2012. Effect of Thickness Variation on the Mechanical Buckling Load in Plates Made of Functionally Graded Materials, Procedia Technology, 1, 2012, p. 496-504.

[18] Oyekoya OO, Mba DU, El-Zafrany AM. 2009. Buckling and vibration analysis of functionally graded composite structures using the finite element method, Composite Structures, 89, 2009, p. 134-142.

[19] Talha M, Singh BN. 2010. Static response and free vibration analysis of FGM plates using higher order shear deformation theory, Applied Mathematical Modelling, 34, 2010, p. 3991-4011.

[20] Shen H-S. Functionally graded materials: nonlinear analysis of plates and shells: CRC press, Boca Raton; 2009.

[21] Roy RK. A primer on the Taguchi method: Van Nostrand Reinhold, New York; 1990.

[22] Ross PJ. Taguchi Techniques for Quality Engineering, 2nd Edition, McGraw-Hill International Book Company, New York; 1996.